

# Metal–Semiconductor–Metal Ultraviolet Photodetectors Based on Zinc-Oxide Colloidal Nanoparticles

Liqiao Qin, Christopher Shing, *Student Member, IEEE*, and Shayla Sawyer, *Member, IEEE*

**Abstract**—Metal–semiconductor–metal ultraviolet (UV) photodetectors were created with zinc-oxide colloidal nanoparticles coated with polyvinyl-alcohol. Gold-interdigitated finger contacts with different parameters were patterned on the nanoparticles by optical lithography. The photodetectors exhibited UV-photogenerated current to dark current ratios ranging from  $3.85 \times 10^6$  to  $1.34 \times 10^8$ , depending on the finger parameters. The spectral responses demonstrate a 375 nm cutoff wavelength, with a peak responsivity of 731.42 A/W at 345 nm.

**Index Terms**—Metal–semiconductor–metal (MSM) ultraviolet (UV) photodetector, optical lithography, polyvinyl-alcohol (PVA), top-down wet-chemical etching, zinc-oxide (ZnO) nanoparticles.

## I. INTRODUCTION

COLLOIDAL nanoparticles are promising in current research due to their 3-D quantum-confinement effects, easy fabrication, large active area, and relatively low cost [1]. As a direct wide-bandgap semiconductor material with large exciton binding energy, zinc oxide (ZnO) is potentially used in optoelectronic devices [1]–[4]. However, ZnO materials usually exhibit a strong parasitic green photoluminescence caused by excess  $\text{Zn}^{2+}$  ions and oxygen deficiencies [5], [6]. Polyvinyl-alcohol (PVA)-coated ZnO nanoparticles created by a top-down wet-chemical means suppressed green emission and used to make high-performance photoconductors were reported in [7]. However, compared with metal–semiconductor–metal (MSM) detectors, photoconductors are limited by longer time responses, larger dark currents, and smaller signal-to-noise ratios.

However, fabrication of reproducible Schottky contacts, particularly high-resolution interdigitated contacts on solution-processed ZnO nanoparticles, is often difficult to achieve. Surface-defect states, residual surface contamination, and the interfacial gap between the metal and semiconductor dominate in nanoparticle devices, causing unpredictability in

Manuscript received September 17, 2010; accepted October 7, 2010. Date of publication November 18, 2010; date of current version December 27, 2010. This work was supported in part by the National Security Technologies through NSF Industry/University Cooperative Research Center Connection One. The review of this letter was arranged by Editor C. Jagadish.

The authors are with the Department of Electrical, Computer, and Systems Engineering, Rensselaer Polytechnic Institute, Troy, NY 12180 USA (e-mail: qinl@rpi.edu; shingc@rpi.edu; sawyes@rpi.edu).

Color versions of one or more of the figures in this letter are available online at <http://ieeexplore.ieee.org>.

Digital Object Identifier 10.1109/LED.2010.2089598

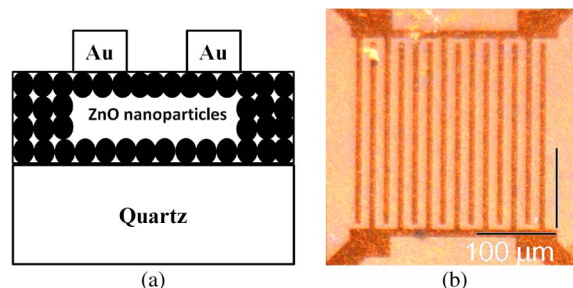


Fig. 1. (a) Structure of ZnO MSM photodetector. (b) Image of interdigitated contacts (7  $\mu\text{m}$  finger width, 10  $\mu\text{m}$  finger spacing, 242  $\mu\text{m}$  finger length, and 250  $\mu\text{m} \times 250 \mu\text{m}$  active area).

current–voltage ( $I$ – $V$ ) characteristics. For example, Jun *et al.* reported a linear  $I$ – $V$  response with gold-metal deposition on the n-type ZnO nanoparticles, although a nonlinear response is expected [1].

In this letter, ZnO-nanoparticle-based MSM photodetectors with different interdigitated electrodes created by traditional optical lithography and wet etching are demonstrated on one quartz substrate. The results show that reproducible high-sensitivity visible blind MSM ultraviolet photodetector based on solution-processed ZnO nanoparticles can be fabricated by using traditional contact patterning and deposition techniques.

## II. EXPERIMENT

ZnO nanoparticles created by a top-down wet-chemistry synthesis process and coated with PVA were dispersed in ethanol to form a 30 mg/ml suspension [7]. This suspension was then spin casted onto a piranha clean quartz plate, with a spin-casting recipe that differed by layers, contributing to a total thickness of about 1.5  $\mu\text{m}$ . The sample was then annealed in air at 150  $^{\circ}\text{C}$  for 5 min. One 176 nm layer of gold was deposited through e-beam on top of the ZnO nanoparticles. Six dies, consisting of 25 pairs of interdigitated electrodes in each die, were transferred to the gold layer through optical lithography and wet etched using gold etchant TFA (produced by Transene, U.S., containing 8 wt% iodine, 21 wt% potassium iodide, and 71 wt% water). The finger parameters of the interdigitated electrodes vary among dies. The schematic diagram of the devices and the image of the interdigitated contacts are shown in Fig. 1. Each die was cut separately by a dicing saw. Finally, each die was packaged and wire bonded utilizing Epo-Tek H20E conductive epoxy.

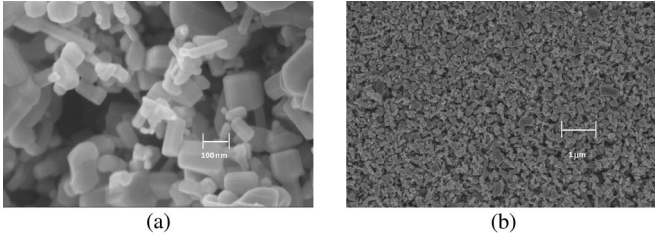


Fig. 2. (a) 100 nm and (b) 1  $\mu\text{m}$  scale resolution SEM images of PVA-coated ZnO.

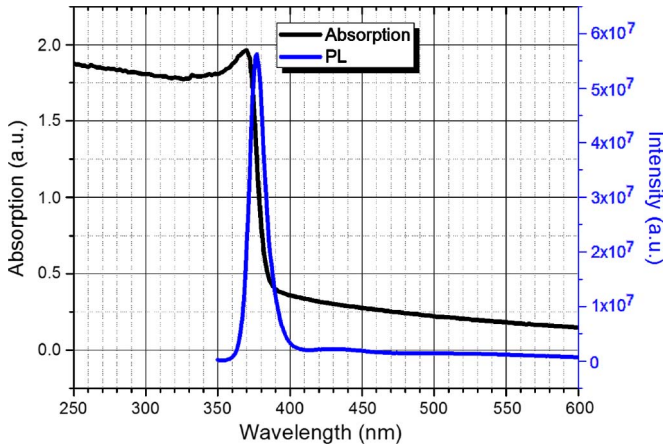


Fig. 3. (Black line) Absorption and (blue line) photoluminescence spectra of PVA-coated ZnO (excited at 340 nm).

### III. RESULTS AND DISCUSSIONS

The 100 nm scale SEM image in Fig. 2(a) shows the size of the PVA-coated ZnO nanoparticles, ranging from 10 to 120 nm with an average size of approximately 80 nm. However, as shown in Fig. 2(b), the nanoparticles distribute uniformly onto the substrate to form a good thin film to conduct currents, although better control about the size distribution of ZnO nanoparticles will result in shorter cutoff wavelength.

The absorption spectrum and photoluminescence of the PVA-coated ZnO nanoparticles are shown in Fig. 3. The cutoff wavelength is 375 nm, with a 5 nm blue shift from the bandgap of ZnO bulk material whose bandgap is 3.26 eV (380 nm). This corresponds to the quantum-confinement effects of nanoparticles [5]–[7]. When excited at 340 nm, the photoluminescence of the ZnO nanoparticles shows a strong ultraviolet (UV) emission with peak at 377 nm (band-edge emission) and a diminished parasitic green emission. The improved UV performance of the ZnO nanoparticles was achieved due to the PVA coating, as it acts as a surface passivation agent. The PVA captures the excess  $\text{Zn}^{2+}$  ions and oxygen deficiencies that contributed to green emission [5]–[7].

Fig. 4 shows a typical  $I$ – $V$  response of an MSM detector (Device #A3 in Table I). The measurements were taken under darkness and illumination from a 340 nm UV LED with an intensity of 45.58 mW/cm<sup>2</sup>. The nonlinear exponential  $I$ – $V$  response indicates that good Schottky contacts with a calculated ideal factor of 1.036 have been created between the PVA-coated ZnO nanoparticles and the gold. The photogenerated current to dark current (on/off) ratio increases sharply once bias voltage is applied. Then, it increases slowly and goes toward saturation.

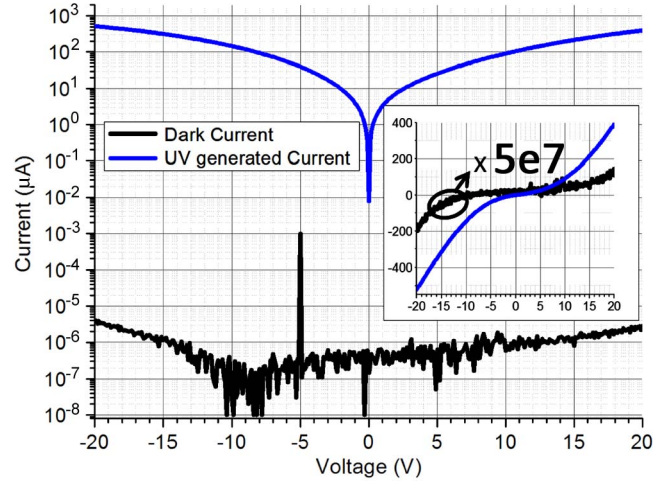


Fig. 4. Typical nonlinear exponential  $I$ – $V$  response of an MSM detector (Device #A3 in Table I) showing an on/off ratio of as high as eight orders.

TABLE I  
PARAMETERS OF EACH DEVICE

Device number	Area	Finger length	Finger width	Finger Spacing	Current Ratio
A5	125 $\mu\text{m}$ $\times$ 125 $\mu\text{m}$	117 $\mu\text{m}$	5 $\mu\text{m}$	5 $\mu\text{m}$	$1.19 \times 10^7$
A6	125 $\mu\text{m}$ $\times$ 125 $\mu\text{m}$	117 $\mu\text{m}$	5 $\mu\text{m}$	7 $\mu\text{m}$	$3.85 \times 10^6$
A8	125 $\mu\text{m}$ $\times$ 125 $\mu\text{m}$	117 $\mu\text{m}$	7 $\mu\text{m}$	5 $\mu\text{m}$	$1.14 \times 10^7$
A7	125 $\mu\text{m}$ $\times$ 125 $\mu\text{m}$	117 $\mu\text{m}$	7 $\mu\text{m}$	10 $\mu\text{m}$	$4.51 \times 10^6$
A2	250 $\mu\text{m}$ $\times$ 250 $\mu\text{m}$	242 $\mu\text{m}$	5 $\mu\text{m}$	7 $\mu\text{m}$	$4.80 \times 10^7$
A3	250 $\mu\text{m}$ $\times$ 250 $\mu\text{m}$	242 $\mu\text{m}$	7 $\mu\text{m}$	10 $\mu\text{m}$	$1.34 \times 10^8$

At 20 V bias, the dark current is 2.91 pA, and the UV-generated current is 391.67  $\mu\text{A}$ , indicating that the ratio of photogenerated current to dark current (on/off ratio) is  $1.34 \times 10^8$ .

Other devices on the same substrate but with interdigitated contact arrays of different finger parameters and active area were also tested. Each tested device demonstrated an MSM nonlinear  $I$ – $V$  response similar to Fig. 4, while the dark currents varied from 1 to 550 pA. As shown in Table I, the on/off ratios are between six and eight orders of magnitude, depending on the finger parameters. Devices with the same active area but decreasing finger spacing exhibit a bigger on/off ratio resulting from the shorter carrier traveling distance. Smaller finger widths also contribute slightly to an on/off ratio increase due to the increase in the effective active area.

Reproducible MSM  $I$ – $V$  characteristics were achieved as a direct result of reducing the surface defects and the interfacial gap between the gold and ZnO nanoparticles. As discussed before, their reduction is attributed to the PVA coating on the ZnO nanoparticles.

Fig. 5 shows the spectral response of an MSM detector (Device #A5 in Table I) under 20 V bias. It demonstrates a normal short-pass performance with a cutoff wavelength at 375 nm and a peak response at 345 nm. The peak response is approximately 731.42 A/W when the optical intensity is 216.46 nW/cm<sup>2</sup>. This high responsivity is attributed to internal photoconductive gain due to the presence of oxygen-related hole-trap states at the nanoparticle surface and the high-resolution interdigitated electrodes. The adsorbed oxygen

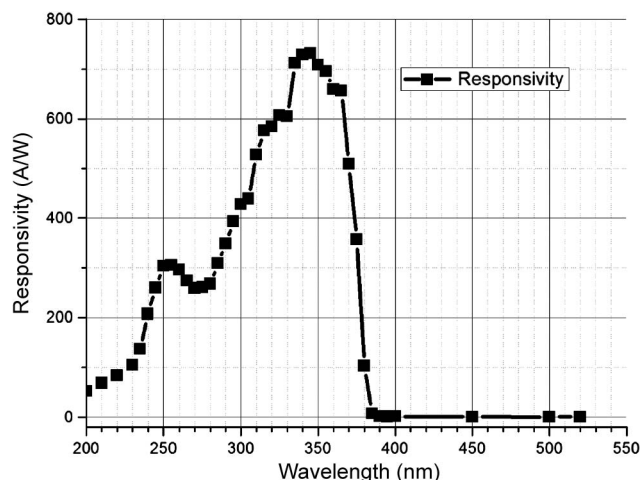


Fig. 5. Spectral response of photodetector (Device #A5, under 20 V bias) with a cutoff at 375 nm and a peak at 345 nm.

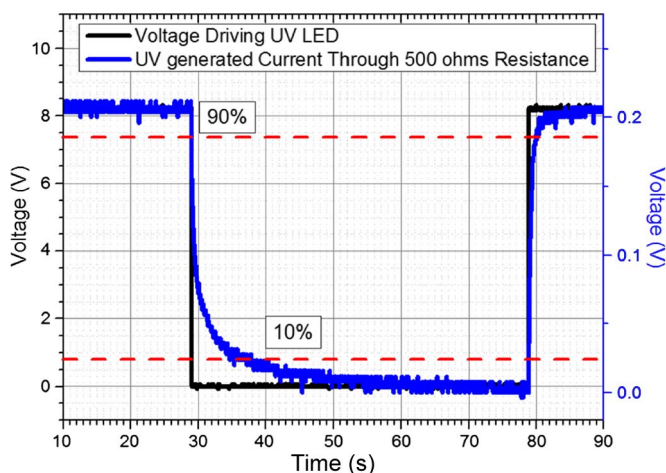


Fig. 6. Time response of photodetector (Device #A8) with a 0.6 s rising time and an 8 s falling time under ambient conditions.

molecules on the ZnO nanoparticles surface capture free electrons to form chemisorbed oxygen [ $O_2(g) + e^- \rightarrow O_2^-(ad)$ ]. When light is absorbed, electron and hole pairs are generated at the nanoparticles surface. The oxygen-related hole-trap states neutralize the chemisorbed oxygen [ $h^+ + O_2^-(ad) \rightarrow O_2(g)$ ] and prevent charge-carrier recombination, prolonging the lifetime of the photocarrier [8]. In addition, the reduced traveling distance of the carriers to the closely spaced finger contacts created by the optical lithography, in comparison with the contacts via shadow mask, also decreases the recombination possibility of the generated carriers.

The time response of the photodetector (Device #A8 in Table I) was measured under a 340 nm UV LED driven by a square-wave signal with a 100 s period. Both the driven signal and the UV-generated current across a 500  $\Omega$  load resistor were measured by an oscilloscope. The result is shown in Fig. 6

from which the rise time (from 10% to 90%) and fall time (from 90% to 10%) of the photodetector extracted are 0.6 and 8 s, respectively. An exponential-decay fitting related to drift and diffusion of electrons/holes according to [9] was performed. The fitting results show that the drift component dominates the rise time with a constant of 0.49 s, while the diffusion component dominates the fall time with a constant of 8.24 s. Further analysis regarding the time response of the different finger parameters will be discussed in greater detail in another paper.

#### IV. CONCLUSION

In conclusion, highly sensitive MSM UV photodetectors based on PVA-coated ZnO nanoparticles and gold interdigitated electrodes patterned by optical lithography have been fabricated. The results indicate that PVA-coated ZnO nanoparticles with reduced surface defects and interfacial gaps contribute to creating reproducible MSM detectors. Large-area planar MSM ultraviolet photodetectors, based on solution-processed ZnO nanoparticles, can be fabricated by using traditional contact patterning and deposition techniques.

#### ACKNOWLEDGMENT

The authors would like to thank Prof. P. Dutta of the Electrical, Computer, and Systems Engineering Department, Rensselaer Polytechnic Institute, for providing the ZnO nanoparticles.

#### REFERENCES

- [1] J. Jun, H. Seong, K. Cho, B. Moon, and S. Kim, "Ultraviolet photodetectors based on ZnO nanoparticles," *Ceram. Int.*, vol. 35, no. 7, pp. 2797–2801, Sep. 2009.
- [2] E. Neshataeva, T. Kümmell, G. Bacher, and A. Ebbers, "All-inorganic light emitting device based on ZnO nanoparticles," *Appl. Phys. Lett.*, vol. 94, no. 9, p. 091115, Mar. 2009.
- [3] S. Lee, Y. Jeong, S. Jeong, J. Lee, M. Jeon, and J. Moon, "Solution-processed ZnO nanoparticle-based semiconductor oxide thin-film transistors," *Superlattices Microstruct.*, vol. 44, no. 6, pp. 761–769, Dec. 2008.
- [4] M. Wang, Y. Lian, and X. Wang, "PPV/PVA/ZnO nanocomposite prepared by complex precursor method and its photovoltaic application," *Curr. Appl. Phys.*, vol. 9, no. 1, pp. 189–194, Jan. 2009.
- [5] Y. L. Wu, A. I. Y. Tok, F. Y. C. Boey, X. T. Zeng, and X. H. Zhang, "Surface modification of ZnO nanocrystals," *Appl. Surf. Sci.*, vol. 253, no. 12, pp. 5473–5479, Jan. 2007.
- [6] L. Wu, Y. Wu, X. Pan, and F. Kong, "Synthesis of ZnO nanorod and the annealing effect on its photoluminescence property," *Opt. Mater.*, vol. 28, no. 4, pp. 418–422, Jun. 2006.
- [7] L. Qin, C. Shing, S. Sawyer, and P. Dutta, "Enhanced UV sensitivity of ZnO nanoparticle photoconductors by surface passivation," *Opt. Mater.*, 2010, DOI:10.1016/j.optmat.2010.09.020.
- [8] C. Soci, A. Zhang, B. Xiang, S. A. Dayeh, D. P. R. Aplin, J. Park, X. Y. Bao, Y. H. Lo, and D. Wang, "ZnO nanowire UV photodetectors with high internal gain," *Nano Lett.*, vol. 7, no. 4, pp. 1003–1009, Mar. 2007.
- [9] E. Monroy, F. Vigu, F. Calle, J. I. Izpura, E. Muñoz, and J.-P. Faurie, "Time response analysis of ZnSe-based Schottky barrier photodetectors," *Appl. Phys. Lett.*, vol. 77, no. 17, pp. 2761–2763, Oct. 2000.